Complex Contagion Influence Maximization: A Reinforcement Learning Approach

Haipeng Chen[1] , **Bryan Wilder**[2] , **Wei Qiu**[3] , **Bo An**[3] , **Eric Rice**[4] , **Milind Tambe**[5]
[1]William & Mary
[2]Carnegie Mellon University
[3]Nanyang Technological University
[4]University of Southern California
[5]Harvard University
hchen23@wm.edu, bwilder@andrew.cmu.edu, qiuw0008@e.ntu.edu.sg,
boan@ntu.edu.sg, ericr@usc.edu, milind_tambe@harvard.edu

Abstract

In influence maximization (IM), the goal is to find a set of seed nodes in a social network that maximizes the influence spread. While most IM problems focus on classical influence cascades (e.g., Independent Cascade and Linear Threshold) which assume individual influence cascade probability is independent of the number of neighbors, recent studies by sociologists show that many influence cascades follow a pattern called complex contagion (CC), where influence cascade probability is much higher when more neighbors are influenced. Nonetheless, there are very limited studies for complex contagion influence maximization (CCIM) problems. This is partly because CC is *non-submodular*, the solution of which has been an open challenge. In this study, we propose the first reinforcement learning (RL) approach to CCIM. We find that a key obstacle in applying existing RL approaches to CCIM is the reward sparseness issue, which comes from two distinct sources. We then design a new RL algorithm that uses the CCIM problem structure to address the issue. Empirical results show that our approach achieves the state-of-the-art performance on 9 real-world networks.

1 Introduction

Influence maximization (IM) is the problem of selecting a subset of *seed* nodes in a social network to maximize the resulting cascade of influence. Such network-based interventions have been applied in many socially important domains such as HIV prevention [Wilder *et al.*, 2021], development [Banerjee *et al.*, 2013], or nutrition campaigns [Kim *et al.*, 2015]. Influence cascades are most commonly modeled using the independent cascade (IC) and linear threshold (LT) models [Kempe *et al.*, 2003]. The key assumption of these models is that influence spreads independently across edges of the network, which may be appropriate for "simple" cascades such as epidemics. However, recent work in sociology shows that collective social behaviors often spread very differently: an individual's behavior is affected by its neighbors as a whole, and "individual adoption was *much more* likely when participants received social reinforcement from multiple neighbors in the social network" [Centola, 2010]. This is explained using the "complex contagion" model [Centola and Macy, 2007], where the adoption probability has a non-concave jump when enough neighbors are activated. Figure 1 shows a comparison of simple vs complex cascade probability to a target node w.r.t. numbers of activated neighbors. There is a noticeable surge at $x = 3$ for complex contagion. Complex contagion has found to be especially important in socially important domains such as the spread of preventative health behaviors [Kuhlman *et al.*, 2011; Centola, 2010] and agricultural innovations in development [Beaman *et al.*, 2021], due to the need to maintain behaviors which are intensive, risky, or dependent on social reinforcement. Designing better interventions in these domains will require algorithms to seed complex cascades.

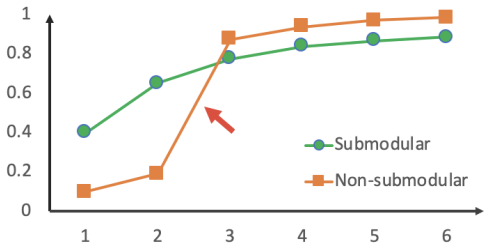

Figure 1: Different trends of influence cascade probability (y-axis) given number of activated neighbors (x-axis), in simple (submodular) vs complex (non-submodular) contagions.

Despite evidence that many influence cascades display complex dynamics [Backstrom *et al.*, 2006; Romero *et al.*, 2011; Ugander *et al.*, 2012], there are very limited studies on CCIM. Mainstream IM algorithms rely crucially on a property of simple contagions called *submodularity*, which intuitively reflects diminishing returns to the selection of additional seeds (the green curve in Figure 1). Under submodularity, a simple greedy algorithm is highly effective [Kempe *et al.*, 2003]. However, the CC models' surge of cascade probability in adoption probability violates submodularity. This greatly complicates optimization by introducing complementarities: the marginal gain to selecting any single seed will often be small since its value is only revealed in combination with a spe-

cific set of other seeds. Formally, this means that CCIM is NP-hard to approximate even under simplified network models [Schoenebeck and Tao, 2019]. To our knowledge, the only practical algorithm for CCIM thus far is the Dynamic Programming for Influence Maximization (DPIM) approach of [Angell and Schoenebeck, 2017]. However, DPIM heavily relies on the assumption that the network has a hierarchical structure and its effectiveness may be limited when a good hierarchical decomposition cannot be found.

CCIM is essentially a stochastic combinatorial optimization problem (COP) with a non-submodular objective function. Inspired by recent works that use RL to address COPs [Bello *et al.*, 2016; Khalil *et al.*, 2017; Kool *et al.*, 2018; Kwon *et al.*, 2020], especially (submodular) influence maximization [Manchanda *et al.*, 2020; Chen *et al.*, 2021], we take a step further and ask the research question: ***Can we use RL to address complex contagion influence maximization?***

The underlying idea of RL-based approaches to COPs is to decompose the original seed *set* selection into a *sequence* of seeds, and it does so greedily based on the marginal "score" of each node. The scores are estimated using deep function approximators. Despite the initial success of applying RL for IM, we found that directly applying these methods to the CCIM problems often yields suboptimal performance. A major challenge is that the reward signal in CCIM is much more sparse than simple contagion IM. We identify two distinct causes of reward sparseness. First, the effective solution space (i.e., solutions with non-negligible influence) is much smaller. This is because CC requires a harsher condition for influence to spread. Second, the marginal contribution of each node (action) in CCIM is more sparse than regular IM, because the reward becomes non-negligible only after multiple seeds are selected. This yields small or zero reward at the first few time steps even with the credit assignment mechanism used in previous works [Manchanda *et al.*, 2020; Chen *et al.*, 2021]. We refer to the two causes of reward sparseness as *effective solution sparseness* and *credit sparseness*.

To address the two issues, we propose a new RL-based solution approach called Reinforcement Learning for Influence Maximization with Complex Contagion (RL4CCIM), with several innovative components to existing approaches [Manchanda *et al.*, 2020; Chen *et al.*, 2021]. For effective solution sparseness, we design a solution filtering step that yields more effective policy exploration. We also use an adapted return-based prioritized experience replay (PER) [Schaul *et al.*, 2016] component that increases the chances of sampling training transitions with higher rewards. For credit sparseness, we propose a new reward-shaping component which, at the end of each training episode, assigns an additional reward to nodes by looking at their marginal contribution w.r.t. the global action sequence.

Our main contributions are: 1) We propose the first learning-based approach to CCIM. Our work is also one of the first few that study CCIM and non-submodular IM. 2) We identify key challenges in applying existing RL approaches to the CCIM problem, and propose a novel RL algorithm to address them. 3) We conduct extensive empirical evaluations. Results on 9 real-world networks and various settings show that our approach achieves state-of-the-art performance. The effectiveness of our proposed components is shown via ablation study.

2 Related Work

Complex contagion influence maximization. [Domingos and Richardson, 2001] are the first to study the IM problem from an algorithmic perspective. [Kempe *et al.*, 2003] formulate it as a discrete optimization problem on the networks, along with a greedy solution which has an approximation ratio of $1 - 1/e$. The greedy algorithm is improved by various follow-up studies [Leskovec *et al.*, 2007b; Borgs *et al.*, 2014; Tang *et al.*, 2015] which accelerate the algorithms with performance guarantees. These studies focus on cascade models such as IC and LT, which are essentially *submodular*. [Backstrom *et al.*, 2006] show that influence diffusion models often appear to be "S-shaped" (see e.g. Figure 1), i.e., the probability of influence propagation has slow growth for small numbers of friends, rapid growth for a moderate numbers of friends, and a rapid flattening of the curve beyond a certain point. The phenomenon is further studied in the epical work [Centola and Macy, 2007] where the *complex contagion* model is introduced to model such collective social behavior, where the cascade probability is higher when multiple neighbors are activated. The model is validated by evidence from various succeeding studies [Leskovec *et al.*, 2007a; Centola, 2010; Romero *et al.*, 2011].[1]

Despite the broad existence of complex contagion, there have been extremely limited studies on the influence maximization problem from an algorithmic perspective. [Ghasemiesfeh *et al.*, 2013; Gao *et al.*, 2016] provide an analytical study of the complex contagion model given certain assumptions of the underlying network models. They do not consider the seed selection problem. [Schoenebeck and Tao, 2017; Schoenebeck and Tao, 2019] point out that the CCIM is non-submodular, and prove that it is NP-hard to approximate even under simplified network models. To our knowledge, [Angell and Schoenebeck, 2017] provide the only practical method that address the non-submodular IM problems via dynamic programming. However, their approach highly relies on the assumption that the networks are hierarchically structured, and therefore its performance heavily depends on the hierarchical decomposition component of the original network. A more recent study [Schoenebeck *et al.*, 2020] prove theoretically the best seeding strategy on the stochastic hierarchical blockmodel, with other strong assumptions on the density of the network. Their seeding strategy has not been empirically evaluated. In contrast to the analytical approaches in existing works, we present the first learning based approach to CCIM.

RL for COPs. The key idea of RL based methods to COPs is to decompose the original combinatorial action into a sequence of individual actions, and then learn policies that greedily select nodes based on the "scores" estimated by deep function approximators [Bello *et al.*, 2016; Graves *et al.*, 2016]. Later approaches integrate RL with more sophisticated representation learning methods such as graph neural networks [Khalil *et al.*, 2017], recurrent neural networks [Nazari *et al.*, 2018], or attention mechanisms [Kool

[1]The other variants of complex contagion [Ugander *et al.*, 2012; Banerjee *et al.*, 2013] are out of scope of this paper.

et al., 2018; Deudon *et al.*, 2018] to better approximate the value/policy functions for COPs. The learning procedures are further augmented by additional beam search [Joshi *et al.*, 2019], Monte Carlo tree search [Fu *et al.*, 2021], dynamic programming [Kool *et al.*, 2021], active search [Hottung *et al.*, 2021], or multiple rollouts during inference [Kwon *et al.*, 2020]. These techniques are then applied in various domains including scheduling in clusters [Mao *et al.*, 2019], transportation [Qiu *et al.*, 2019], job shop scheduling [Zhang *et al.*, 2020], vehicle routing [Kool *et al.*, 2021], network planning [Zhu *et al.*, 2021] and epidemics control [Ou *et al.*, 2021]. We refer to [Bengio *et al.*, 2021; Mazyavkina *et al.*, 2021] for a detailed survey.

RL for IM. Early attempts of RL for IM problems [Lin *et al.*, 2015; Ali *et al.*, 2018] focus on learning which high-level greedy algorithm to use, instead of the specific seeding strategy. [Kamarthi *et al.*, 2020] apply RL to explore the structure of an unknown network in influence maximization, instead of the seeding strategy. [Li *et al.*, 2019; Tian *et al.*, 2020; Manchanda *et al.*, 2020; Chen *et al.*, 2021] extend the method in [Khalil *et al.*, 2017] to address the IM problem, where to address the credit assignment problem, the reward of a new node is defined as its marginal contribution. [Manchanda *et al.*, 2020] focus on solving IM problem instances with very large networks. [Chen *et al.*, 2021] use RL to address IM problem where the willingness of a node to be a seed is uncertain. To the best of our knowledge, none of them consider CCIM, which is much more challenging compared to classic IM because of non-submodularity and the resulting reward sparseness issues.

3 Complex Contagion Influence Maximization

We consider a social network as a graph $G = (V, E)$, where V and E are the nodes and edges, respectively. Each node is either *activated* or *inactivated*, which means the node is influenced or not. We assume all nodes are initially inactivated unless chosen as the seed node. Nodes which are linked by edges have a probability p of influencing each other. For each node v, its neighbors are represented as $\mathcal{N}(v)$. In simple contagions such as the Independent Cascade (IC) model [Goldenberg *et al.*, 2001] and the Linear Threshold (LT) model [Granovetter, 1978], the probability p is assumed to be a constant that is independent of the number of its neighbors[2]. In complex contagion, the assumption is relaxed, and p is represented as a dependent variable of the number of activated neighbors k. Without loss of generality, we consider the most classical K-complex contagion model [Centola and Macy, 2007; Centola, 2010; Ghasemiesfeh *et al.*, 2013], where

$$p(k) = \begin{cases} p_0, & \text{if } k \geq K \\ p_1, & \text{if } k < K \end{cases} \tag{1}$$

where $0 \leq p_1 \ll p_0 \leq 1$. p_1 (p_0) can be interpreted as a very small (large) influence probability when there is a small (large) number of activated neighbors. $K \geq 1$ is an integer threshold value. K is interpreted as the threshold to make a qualitative change to $p(k)$. Given a set $S \subseteq V$ of seed nodes, the influence of the complex contagion is represented as $\sigma(G, S)$. The complex contagion influence maximization problem is to select the optimal set of seeds S^* such that the influence is maximized:

$$S^* = \arg\max_{S \subseteq V} \sigma(G, S) \tag{2}$$

given $|S| = T$, i.e., the number of seeds is equal to budget T.

Definition 1. *A set function $f : 2^V \to \mathbb{R}$ is submodular if for any $S \subset S' \subset V$ and any $v \in V \setminus S'$, it holds that*

$$f(S \cup \{v\}) - f(S) \geq f(S' \cup \{v\}) - f(S')$$

Theorem 1. *The influence function $\sigma(G, S)$ defined based on the cascade probability function in Equation.*(1) *is non-submodular.*

See proof in Appendix A. Because Independent Cascade (IC) IM is NP-hard [Kempe *et al.*, 2003], we have

Theorem 2. *The K-complex contagion influence maximization problem is NP-hard.*

The proof can be done by showing that a special instance of K-complex contagion is an *arbitrary* instance of the IC model. Consider a *special* instance of K-complex contagion when $K = 1$. In this instance, the cascade probability $p(k)$ in Eq.(1) becomes a constant value that does not depend on k: $p(k) = p_0$. In other words, it is equivalent to an *arbitrary* instance of the IC model.

Non-submodular models are fundamentally harder than submodular ones because the algorithm needs to take exactly the right *combination* of nodes before receiving any reward; the individual actions may fail to generate any influence on their own. For submodular models, there are no such "complementarities" between nodes and so greedy strategies are provably optimal. An advantage of RL over other heuristics is that during training it looks ahead multiple steps (guided by the exploration policies, the n-step return, and the intermediate rewards we propose) instead of being trapped in a bad local optimum like greedy methods. Another strength of RL is that it can learn policies to any given network structure without redesigning the solution architecture.

Therefore, inspired by recent works that combine RL and graph representation techniques to address COPs on graphs [Khalil *et al.*, 2017; Deudon *et al.*, 2018; Bengio *et al.*, 2021] and influence maximization in particular [Manchanda *et al.*, 2020; Chen *et al.*, 2021], we design a new RL algorithm to address the CCIM problem, called Reinforcement Learning for Complex Contagion Influence Maximization (RL4CCIM).

4 MDP Formulation & RL Preliminary

4.1 MDP Formulation of CCIM

In order to fit the complex contagion influence maximization problem into the RL framework, we first formulate this problem as a discrete time MDP. In this MDP, the *time steps* $t = 1 \dots T$ correspond to the sequence of seed node selections. That is, each time step t means selecting one seed node, and the *time horizon* of the MDP is the total budget T.

[2]By LT, we refer to the canonical version where the activation threshold is uniformly distributed in [0,1], which is submodular. In LT models, p can be seen as the weight that an activated neighbor adds to the target node.

The *state* captures the current status of a node selection time step t, i.e., which nodes have already been selected before t. We use a binary indicator vector $X_t \in \{0,1\}^{|V|}$ to represent the state, where an element $X_{t,v} = 1$ means the node v is selected (activated), and 0 otherwise. It is easy to see that $\sum_{v=1}^{|V|} X_{t,v} = t-1$, i.e., the total number of selected nodes at time t is equal to $t-1$. Here X_t can be seen as the vector-form equivalence of the set-form notation S_t (i.e., the set of nodes selected as seeds at time t).

Given state X_t at time t, the *action* a_t is to select the next node. We use a one-hot vector $a_t \in \{0,1\}^{|V|}$ to represent the action, where the non-zero element $a_{t,v} = 1$ means node v is the selected node at the current time step. The *transition function* is represented as

$$X_{t+1} = X_t + a_t \tag{3}$$

It is worth noting that the transition function in this setting is deterministic. The *terminal state* X_T is the state at the final time step T, and it suffices that $\sum_{v=1}^{|V|} X_{T,v} = T$. Following the ideas in [Manchanda *et al.*, 2020; Chen *et al.*, 2021], the one-step reward is defined as the marginal contribution of a new seed node selected at time t, i.e.,

$$r(X_t, a_t) = \sigma(G, X_{t+1}) - \sigma(G, X_t) \tag{4}$$

where $\sigma(G, X_t)$ is equivalent to the set-form notation $\sigma(G, S_t)$, with S_t being the set of seeds selected at t.

4.2 RL Preliminaries

RL is a learning paradigm where *agents* learn to take actions in an *environment* to achieve a certain *goal*. In this paper, the environment is the MDP that we formulated previously. At each time step t of the MDP, the agent takes an *action* based on its *policy* $\pi(a_t|X_t)$, where X_t and a_t are respectively the state and action of the MDP. The selected action then interacts with the environment and the environment returns a *reward* signal $r_t(X_t, a_t)$ which reflects how good the action/policy is, as well as the next state X_{t+1}. Q-learning [Watkins and Dayan, 1992] is a value-based RL variant that represents the value of a state action pair (X_t, a_t) with the *Q-function* $Q(X_t, a_t)$. The Q-function is usually updated using the Bellman equation: $Q(X_t, a_t) = r_t(X_t, a_t) + \gamma \max_{a_{t+1}} Q(X_{t+1}, a_{t+1})$, where γ is the discount factor. During training, actions are usually taken by balancing the *exploitation* which takes the action with the highest Q-value, and *exploration* which takes a random action (usually with a decaying probability ε). DQN [Mnih *et al.*, 2013] improves Q-learning's function approximator with parameterized deep neural networks $Q_\theta(X_t, a_t)$, together with adoption of other techniques including the ideas of experience replay [Lin, 1992], which stores the training trajectories in a replay buffer and then updates the neural networks parameters θ using mini-batches of data. In this paper, we use the double-DQN framework [Van Hasselt *et al.*, 2016] as our base RL method which trains an additional *target* network to mitigate the overestimation issue in vanilla DQN.

5 RL4CCIM

We first use a motivating example that illustrates the reward sparseness issues. We then introduce the key methodology.

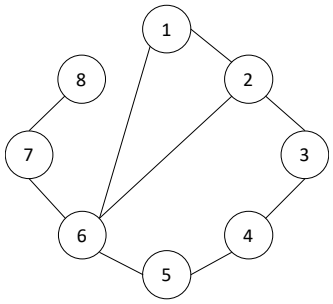

Figure 2: An example network.

5.1 A Motivating Example

Recent studies [Khalil *et al.*, 2017; Kwon *et al.*, 2020] integrate RL with deep function approximators to address combinatorial optimization over graphs, including influence maximization [Manchanda *et al.*, 2020; Chen *et al.*, 2021]. We build RL4CCIM on this line of works. Despite the initial success of these methods in generic COPs and IM problems, we found that the non-submodularity of the CC models and the resulting *reward sparseness* creates a major hurdle that prevents us from directly applying these existing methods.

More specifically, the reward sparseness arises from two causes: the *effective solution sparseness* and *credit sparseness*. To take a closer look at the two issues, we refer to the example network in Figure 2 with a standalone illustration. Set $p_0 = 1$, $p_1 = 0$, $K = 3$ in Eq.(1), and the budget as $T = 4$. There are in total $C_8^4 = 70$ feasible solutions. (i) **Effective solution sparseness**. For simple contagion (i.e., $K = 1$) where $p(k) = p_0 = 1$, because it is a fully connected network, any solution is an effective solution. Whereas for the complex contagion ($K = 3$), only nodes 2 and 6 have at least 3 neighbors, and therefore can be activated when there are enough activated neighbors. Many solutions (e.g., $\{5,6,7,8\}$ or $\{1,2,3,4\}$) are ineffective which cannot activate any other node. Using exhaustive search, we can get that there are 17 out of $C_8^4 = 70$ combinations of 4 seeds that are effective solutions, taking up only 24.3%. (ii) **Credit sparseness**. We consider a sequence of seed nodes: $\{1,2,3,5\}$. It is an effective solution which can activate node 6. However, because of the way the reward is defined (see Eq.(4)), the reward of the first three steps are all 1's (i.e., only the seed node itself is activated), and only the last time step has a reward of 2. This leads to very slow training since the first time steps yield the same reward of 1.

5.2 RL4CCIM Architecture

The above two issues motivate the design of RL4CCIM. Figure 3 shows the overall architecture of RL4CCIM, where the key novelties are i) a solution filtering mechanism that provides a warm-start of the learning procedure, ii) a customized prioritized experience replay component that encourages training transitions with higher rewards, and iii) a reward shaping component which mitigates the assignment sparseness issue. Algorithm 1 presents the training algorithm of RL4CCIM, which follows the flow of DQN, with the 3 new elements being described in: Lines 3-5 and 9 for solution filtering, Line 11 for PER, and Lines 13-16 for reward shaping.

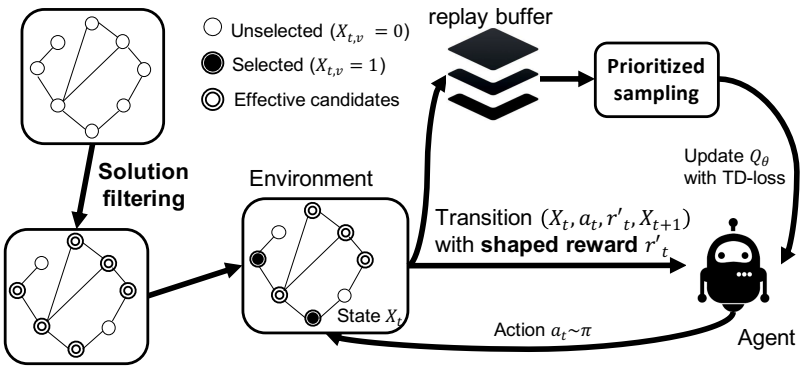

Figure 3: RL4CCIM architecture. It starts by solution filtering as a pre-processing step which filters out all effective candidates $\mathcal{A}$. After that, learning starts by going over multiple episodes where the agent and the environment iteratively interacts and generates training transitions. The generated transitions with the shaped reward r'_t are periodically stored in the replay buffer, and the prioritized sampling unit then samples mini-batches of transitions to update Q_θ, which is subsequently used to generate more actions and training transitions.

As a fourth improvement, instead of using S2V [Dai *et al.*, 2016] as the function approximator that works as the graph representation learning unit in [Khalil *et al.*, 2017] and RL4IM [Chen *et al.*, 2021], we use a more advanced graph representation learning technique called graph attention networks (GAT) [Veličković *et al.*, 2018]. GAT is a neural network architecture that operates on graph-structured data, leveraging masked self-attentional layers [Vaswani *et al.*, 2017] to address the shortcomings of prior methods based on graph convolutions or their approximations. We focus on the elaboration of the first three improvements and refer to the original paper [Veličković *et al.*, 2018] for a detailed description of GAT.

Algorithm 1: RL4CCIM training

1 **Input:** network $G = (V, E)$, seed budget T, complex contation paramters p_0, p_1, K
2 Initialize $Q_\theta(\cdot)$ and replay buffer $\mathcal{M} \leftarrow \emptyset$
3 Initialize $\mathcal{A} \leftarrow \emptyset$
4 **for** $v \in V$ **do**
5 **if** $|\mathcal{N}(v)| \geq K$ **then** $\mathcal{A} \leftarrow \mathcal{A} \cup \mathcal{N}(v)$;
6 **for** *episode* $= 1 \dots \mathcal{E}$ **do**
7 Reset environment, initialize state $X_1 \leftarrow 0$
8 **for** $t = 1 \dots T$ **do**
9 With probability $1 - \varepsilon$ take action $a_t \leftarrow \arg\max_{a_t \in} Q_\theta(X_t, a_t)$; with probability $\varepsilon * \varepsilon'$ take a random action $a_t \in \{0,1\}^{|\mathcal{A}|}$; with probability $\varepsilon(1 - \varepsilon')$ take a random action $a_t \in \{0,1\}^{|V|}$
10 Get new transition $m \leftarrow (X_t, a_t, r_t, X_{t+1})$, where r_t is calculated with Eq.(4).
11 Sample mini-batch data $M \subset \mathcal{M}$ with Eq.(5)
12 Update Q_θ with M using gradient descent
13 **for** $t = 1 \dots T$ **do**
14 Calculate $r'(X_t, a_t)$ with Eq.(7)
15 Get shaped transition $m' \leftarrow (X_t, a_t, r'_t, X_{t+1})$
16 Update replay buffer $\mathcal{M} \leftarrow \mathcal{M} \cup m'$
17 **return** $Q_\theta(\cdot)$

5.3 Solution Filtering

As introduced previously, a main challenge in applying existing RL for IM methods is the effective solution sparseness.

Definition 2 (*Effective solution*)**.** *Given G and $\sigma(G, S)$, an effective solution is a solution S where $\sigma(G, S) > |S|$.*

For a network $G = (V, E)$ and a budget of T, the size of the feasible solution space is then $C^T_{|V|}$, the complexity of which is $O\big(\min(|V|^T, |V|^{|V|-T})\big)$. While the sequence decomposition avoids enumerating the combinatorial action space, the effective solutions are in fact very sparse in the CCIM problem. This makes initial learning very slow as most episodes have close to 0 rewards. For instance, only 24.2% of nodes in the toy example in Figure 2 have non-zero rewards. The percentage of effective solutions gets even lower when the network sizes and the threshold K are larger.

To that end, our key observation is that certain nodes are never part of an effective solution. For example, nodes 4 and 8 are never able to activate any other nodes. Thus, we may remove them from the feasible solution space to increase the chances that effective solutions are selected. In doing so, the number of feasible solutions becomes $C^4_6 = 15$, which is $15/70 = 21.4\%$ of the original feasible solution space.

Inspired by this, we design a *solution filtering* mechanism, as described in Lines 3-5 of Algorithm 1. We initialize an empty node set $\mathcal{A} = \emptyset$ which stores the set of filtered nodes that could potentially be selected as seed nodes. We enumerate through each node $v \in V$ of a network, and check if the number of its neighbors is no smaller than the threshold K. If it is, then we update $\mathcal{A}$ as the union of $\mathcal{A}$ and all the *neighbors* of v. In this case, if a node is not in *any* neighborhood which can potentially activate another node, that node will not be contained in the effective candidate set $\mathcal{A}$. Because of this, it is guaranteed that

Theorem 3. *The effective candidate set $\mathcal{A}$ contains any effective solution S where $\sigma(G, S) > |S|$.*

This means that the solution filtering step does not exclude *any* potentially optimal solution. When exploring new actions, instead of taking a random action from the entire action space

$\{0,1\}^{|V|}$, the action exploration in RL4CCIM is initially restricted on $\{0,1\}^{|\mathcal{A}|}$ (Line 9). To ensure that the solution space is sufficiently explored and un-biased in the final stage, we use an annealing factor (similar to the original exploration probability ε) ε' that gradually deceases from a large value (e.g., 0.99) to a small value (e.g., 0). The probability of selecting from the effective candidate set $\mathcal{A}$ is then $\varepsilon * \varepsilon'$.

5.4 Reward-based Prioritized Experience Replay

The solution filtering mechanism does not guarantee that any combination of solution in $\mathcal{A}$ is effective. E.g., in Figure 2, if there is a node 9 which is only linked to node 3, then $\mathcal{A} = \{1,2,3,4,5,6,7,9\}$. However, solution $\{1,2,6,9\}$ does not activate any other node and thus is not an effective solution.

The solution filtering mechanism works at the generation time of training trajectories. All the transitions generated will be stored into the replay buffer and later used to sample batches of training data. To further encourage sampling effective solutions, or more specifically, solutions with higher rewards, we adopt the idea of Priotized Experience Replay (PER) [Schaul *et al.*, 2016]. Opposed to sampling transition data uniformly in classical experience replay [Lin, 1992], PER samples transition data with different priorities defined based on a certain metric.

In [Schaul *et al.*, 2016], the selection metric is defined as the temporal difference (TD) error $\delta = r_t(X_t, a_t) + \gamma \max_{a_{t+1}} Q(X_{t+1}, a_{t+1}) - Q_\theta(X_t, a_t)$. Let $q_i = |\delta_i| + \epsilon$, where $\epsilon > 0$ is a very small value to prevent 0 in the denominator, the probability of sampling a trajectory i with TD error δ_i is then $P_i = \frac{q_i^\alpha}{\sum_k q_k^\alpha}$, where α is a temperature parameter.

In RL4CCIM, because we aim to increase the chances of sampling transitions with higher rewards, we propose two other versions of priority values. One version is to directly use reward[3] $r_i(X, a)$ as the priority value: $p_i = r_i(X, a) + \epsilon$. Though this encourages transitions with higher rewards, it has the risk of causing *overestimation*, where the biases of rewards are exaggerated by the Bellman target [Van Hasselt *et al.*, 2016]. Indeed, we found that in practice, this version is sometimes not stable. We therefore introduce a third variant which takes the (weighted) sum of them $q_i = |\delta| + \beta r_i(X, a) + \epsilon$. The sampling probability is then:

$$P_i = \frac{(|\delta|_i + \beta r_i(X, a) + \epsilon)^\alpha}{\sum_k (|\delta_k| + \beta r_k(X, a) + \epsilon)^\alpha} \tag{5}$$

This form of priority balances the benefit of training with high reward transitions and the risk of overestimating Q values.

5.5 Reward Shaping

As shown in Eq. (4), existing RL for IM methods define the reward of a new seed node a_t as the marginal contribution of that node w.r.t. its "preceding" seeds $X_t = \sum_{\tau=1}^{t-1} a_\tau$. This is reasonable when the influence function is submodular – because the following nodes will make smaller marginal contributions. This becomes insufficient when it comes to complex contagion, where the influence function is no-longer submodular. As illustrated in Section 5.1, this incurs the credit sparseness issue.

To mitigate this issue, our idea is to add a regularization term to the reward, which accounts for its marginal contribution (which is much more likely to be non-zero) from a "global" perspective. At first thought, the most desirable regularization is the Shapley value [Shapley, 2016]. This, however, introduces exponentially large number of calculations of marginal contributions, which is computationally infeasible. As a simplified alternative, we use the marginal contribution of action a_t w.r.t. the sequence of nodes selected in the same episode:

$$r_{global}(s_t, a_t) = \sigma(G, a_{1:T}) - \sigma(G, a_{1:t-1}; a_{t+1:T}) \tag{6}$$

where $a_{1:t} \coloneqq \sum_{\tau=1}^{t} a_\tau$. $a_{1:t-1}$ and $a_{t+1:T}$ respectively represent preceding and proceeding seed nodes of a_t. The shaped reward is then represented as:

$$r'(X_t, a_t) = r(X_t, a_t) + \omega \cdot r_{global}(X_t, a_t) \tag{7}$$

where ω is the weight. Note that this requires running an entire simulation before assigning the immediate reward of each action/seed (see Lines 13-16 of Algorithm 1).

6 Experiments

We first present evaluations of the performances of RL4CCIM and baselines on various real-world networks and problem settings. We then do an ablation study to evaluate the effectiveness of the components that we introduce in Section 5. All experiments are run on a Dell DSS 8440 Cauldron node, with a virtual environment, 2 Intel Xeon Gold 6148 2.4G CPU cores, 5G RAM, 1 NVIDIA Tesla V100 32G GPU, EDR Infiniband.

We consider the following baselines: (i) **Random+**, which selects seeds randomly from the effective candidate set $\mathcal{A}$, (ii) **Greedy** [Kempe *et al.*, 2003], which is the prominent approach for submodular IM, (iii) **DPIM** [Angell and Schoenebeck, 2017], which is a dynamic programming based method designed for non-submodular IM including CCIM. To the best of our knowledge, this method is the only published method for non-submodular IM. Note that the code of DPIM is not publicly available. Therefore we implemented our own version of DPIM, where to build a hierarchical decomposition tree of the original network, we use the Jaccard Similarity variant (see Section 4.1.3 of [Angell and Schoenebeck, 2017]). Our implementation of DPIM is in the supplementary material, and we plan to open-source it at the time of publication. (iv) **RL4IM** [Chen *et al.*, 2021], which is the most recent work that uses RL for submodular IM.The hyper-parameter values selected and ranges that are searched within for different methods are described in Appendix B.

To have a sense of the optimality gap of the different methods (on small networks), we also implemented a Mixed Integer Programming (**MIP**) based optimization approach (shown as the last row "**OPT**" of Table 1) using the Gurobi solver. The detailed description of the formulation is in Appendix D. While MIP finds the exact optimum, its runtime increases rapidly with the network size. We set a 12 hour time limit, which was exceeded starting at Network SPY (67 nodes). We also found that in stochastic settings MIP was too expensive

[3] In practice, we use the "n-step" return [Watkins, 1989] instead because it can look at more steps of reward in the future, but omit the discussions here for ease of reading.

Method \ Network	CHANGE	DC	DOSIM	MFP	SPY	Football	Polbooks	India	Exhibition
Greedy	0.1509	0.3902	0.225	0.3194	0.4925	0.3217	0.4571	0.0396	0.0293
DPIM	**0.283**	0.4146	0.35	0.2917	0.477	0.3913	0.6762	0.3911	0.5537
Random+	0.1632	0.3049	0.2175	0.1313	0.2955	0.0926	0.1486	0.0498	0.0293
RL4IM	**0.283**	0.4146	0.325	0.3194	0.4925	0.513	0.7429	0.3465	0.5439
RL4CCIM	**0.283**	**0.4634**	**0.375**	**0.3472**	**0.5075**	**1.0**	**0.819**	**0.5347**	**0.5585**
OPT	0.3019	0.4634	0.375	0.375	0.5522	N/A	N/A	N/A	N/A

Table 1: Normalized influence of different methods on 9 real-world networks. Best results (except OPT) are highlighted.

to solve even for small networks. This shows that CCIM is too difficult for existing generic optimization approaches.

We evaluate different methods on a set of 9 real-world networks. These include 5 small social-networks that are collected from homeless youth shelters in the city of Los Angeles. They are denoted as **CHANGE, DC, DOSIM, MFP, SPY**. We also evaluate on 4 publicly available and larger sized real-world networks, including **Football** [Girvan and Newman, 2002], **Polbooks** [Rossi and Ahmed, 2015], **India** [Banerjee *et al.*, 2013], and **Exhibition** [Isella *et al.*, 2011]. The detailed description of the networks is presented in Appendix C. Note that training time and scalability are not the focus of our work, so all experiments are run on small-sized networks. Training of all RL-based methods finishes within 2 hours.

6.1 Comparing with Baselines

In the basic problem setting, we set propagation probabilities $p_1 = 0, p_0 = 1$, so that the propagation is deterministic. This setting is convenient for comparison as it rules out the factor that arises from stochasticity of different runs. We will show results later in a setting with stochastic propagation. The threshold K values are set to 3 for small networks CHANGE-SPY, 4 for medium networks (Football, Polbooks and India), and 6 for the largest network Exhibition. The values are set as such so that the influence spread is neither too sparse (very few nodes are influenced) nor too dense (most nodes are influenced) where comparisons become trivial. In this set of experiments, we set the seed budget $T = 8$ for all the networks except for the largest network Exhibition which is $T = 12$. In deterministic settings, there is no randomness for Greedy and DPIM. Randomness of Random+ and RL methods arises from different running seeds. For Random+, we run 50 times each and take the average. For RL methods, we run 15 times and find the best model via a separate validation process (performs every 20 training time steps), and report its performance.

We have these observations in Table 1. (i) **RL4CCIM consistently obtains the best results among all the methods across all the 9 networks.** It obtains the optimal or close-to-optimal solutions on small networks. (ii) The Random+ method, though being far from optimal, seems to be sufficient to serve as a warm-start for RL4CCIM. (iii) Surprisingly, **Greedy can be arbitrarily bad**. For example, Greedy obtains only an influence value of 0.0396 on the India network. Considering that there are 202 nodes in this network, this means that Greedy does not find any effective solution. To better understand this, we compare the seeds selected by Greedy and RL4CCIM on the India network in Figure 6 of Appendix E. (iv) **RL4IM and DPIM are unstable.** RL4IM achieves influence values close to RL4CCIM on some networks (e.g., CHANGE, SPY, and Exibition). However, on some other networks, especially relatively large networks (Football, Polbooks, and India), it is significantly beaten by RL4CCIM. Our hypothesis is that the effective solution sparseness becomes more severe when the entire solution space grows larger. The same holds for DPIM, where it works well on networks such as CHANGE and Exhibition, but is much worse than RL4CCIM on some other networks (e.g., Football and India). A main reason, in our understanding, is that DPIM highly relies on the assumption that networks are hierarchically structured, and therefore the performance of it highly depends on how the network's structure is aligned with the assumption. Unfortunately in practice, it is hard to measure the hierarchy of networks.

6.2 Evaluation on Various Other Problem Settings

We are also interested to see how different methods work under a variety of other problem settings, including: (a) **Stochastic propagation.** We set the range of p_1 as $[0.2, 0.4, 0.6, 0.8, 1]$. In the stochastic setting, we also run Greedy and DPIM for 20 times and report the average. (b) **Seed budget T.** We set the range of T as $[6, 8, 10, 12, 14]$. (c) **Activation threshold K.** We set its range as $[2, 3, 4, 5, 6]$. When evaluating changing T in Football, we set $K = 5$ instead of 4 as $k = 4$ immediately yields influence value of 1 for RL4CCIM (see for example Figure 4f) and thus the comparison becomes trivial.

We evaluate the different settings on three networks, including India, Football, and Polbooks. The results are shown in Figure 4. We can notice that the trends on different networks are consistent. For example, Figures 4(a)-(c) show the results on the India network. We can see that: (i) In all of the settings, **RL4CCIM still consistently outperforms all the baselines.** This shows the robustness of RL4CCIM. (ii) It follows the intuition that the influence value is higher when there is a higher propagation probability p, a larger number of seeding budget T, and a smaller threshold K. (iii) Interestingly, there is a surge of influence value for Greedy when the seed budget T increases from 12 to 14, and when the threshold K decreases from 4 to 3. Our hypothesis is that when T becomes larger (or K becomes smaller), the ratio of effective solutions becomes much larger, and therefore the estimation of marginal influence w.r.t. a *set* of nodes for Greedy becomes much more accurate. However, both of the situations essentially come at the cost of a large seed budget.

6.3 Ablation Study

To evaluate the effectiveness of the different customized components, we also conduct an ablation study on the India network, using the basic problem setting. In each comparison,

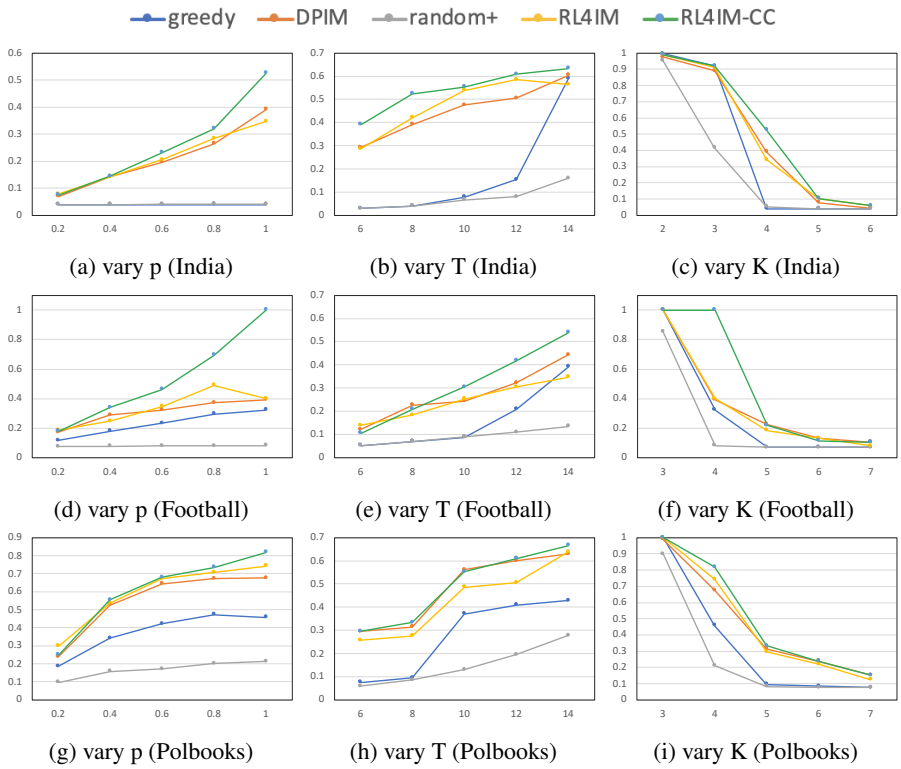

(a) vary p (India) (b) vary T (India) (c) vary K (India)

(d) vary p (Football) (e) vary T (Football) (f) vary K (Football)

(g) vary p (Polbooks) (h) vary T (Polbooks) (i) vary K (Polbooks)

Figure 4: Performance of different methods under various settings, on networks India, Football and Polbooks. The x-axis is the value of the underlying parameter being evaluated, and the y-axis is the normalized influence.

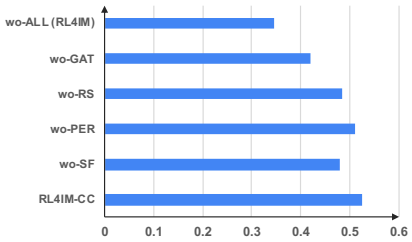

Figure 5: Ablation study. The x-axis is the normalized influence.

we remove one of the 4 components, and get 4 versions of RL4IMC-CC, namely 1) wo-SF (without solution filtering), 2) wo-PER (without prioritized experience replay), 3) wo-RS (without reward shaping), 4) wo-GAT ((without GAT, using S2V instead). Finally, we also show the version without any of these components (wo-ALL), which reduces to RL4IM. The comparison is shown in Figure 5. We can see that by removing each of the components, there is a substantial decrease in the normalized influence value, respectively 10.2% (wo-SF), 4.6% (wo-PER), 9.3% (wo-RS), and 21.3% (wo-GAT). When removing the 3 components altogether, there is a largest decrease of 35.2%. These results demonstrate the importance of all the four additional components.

Limitation Though our method works well on the smaller networks, scalability is a major limitation of the current version. The main bottlenecks of scaling up are (roughly) two-fold: (1) Simulation time of complex contagion. Simulation time is the top bottleneck as RL needs sufficient training episodes. For simple contagion models which are much better studied, there have been efficient methods that can accelerate the simulation (e.g., [Wang *et al.*, 2012]). Complex contagion on the contrary, has been less studied. Hence less effort has been put on improving the simulation efficiency of complex contagion, partly also due to the fact that complex contagion is more challenging to simulate. (2) RL training. On the other hand, gradient updates in Q-networks take more time and memory as it requires larger scale matrix computation. To overcome this issue, a solution is to do pre-processing of the large networks. For example, we may scale them down by pruning less important/informative nodes from the original networks (e.g., the idea from [Manchanda *et al.*, 2020]).

7 Conclusion

We propose the first learning-based approach to CCIM, with multiple innovative components that exploit the structure of the CCIM problem. Empirical results show that our approach achieves new state-of-the-art performance in CCIM. Our work opens up many potential future directions for learning-based approach to CCIM. For example, it is interesting to explore: (i) Can we design more efficient RL algorithms for *larger networks*? (ii) Can the learned RL policies *generalize* to new networks? (iii) What if the network structures or the complex contagion model parameters are uncertain?

Acknowledgments

This work was supported by the Army Research Office (MURI W911NF1810208). Bo An is supported by the National Research Foundation, Singapore under its Industry Alignment Fund – Pre-positioning (IAF-PP) Funding Initiative. Any opinions, findings and conclusions or recommendations expressed in this material are those of the author(s) and do not reflect the views of National Research Foundation, Singapore.

References

[Ali *et al.*, 2018] Khurshed Ali, Chih-Yu Wang, and Yi-Shin Chen. Boosting reinforcement learning in competitive influence maximization with transfer learning. In *WI*, pages 395–400, 2018.

[Angell and Schoenebeck, 2017] Rico Angell and Grant Schoenebeck. Don't be greedy: Leveraging community structure to find high quality seed sets for influence maximization. In *WINE*, pages 16–29. Springer, 2017.

[Backstrom *et al.*, 2006] Lars Backstrom, Dan Huttenlocher, Jon Kleinberg, and Xiangyang Lan. Group formation in large social networks: Membership, growth, and evolution. In *KDD*, pages 44–54, 2006.

[Banerjee *et al.*, 2013] Abhijit Banerjee, Arun G Chandrasekhar, Esther Duflo, and Matthew O Jackson. The diffusion of microfinance. *Science*, 341(6144), 2013.

[Beaman *et al.*, 2021] Lori Beaman, Ariel BenYishay, Jeremy Magruder, and Ahmed Mushfiq Mobarak. Can network theory-based targeting increase technology adoption? *American Economic Review*, 111(6):1918–43, 2021.

[Bello *et al.*, 2016] Irwan Bello, Hieu Pham, Quoc V Le, Mohammad Norouzi, and Samy Bengio. Neural combinatorial optimization with reinforcement learning. *arXiv preprint arXiv:1611.09940*, 2016.

[Bengio *et al.*, 2021] Yoshua Bengio, Andrea Lodi, and Antoine Prouvost. Machine learning for combinatorial optimization: A methodological tour d'horizon. *European Journal of Operational Research*, 290(2):405–421, 2021.

[Borgs *et al.*, 2014] Christian Borgs, Michael Brautbar, Jennifer Chayes, and Brendan Lucier. Maximizing social influence in nearly optimal time. In *SODA*, pages 946–957, 2014.

[Centola and Macy, 2007] Damon Centola and Michael Macy. Complex contagions and the weakness of long ties. *American Journal of Sociology*, 113(3):702–734, 2007.

[Centola, 2010] Damon Centola. The spread of behavior in an online social network experiment. *Science*, 329(5996):1194–1197, 2010.

[Chen *et al.*, 2021] Haipeng Chen, Wei Qiu, Han-Ching Ou, Bo An, and Milind Tambe. Contingency-aware influence maximization: A reinforcement learning approach. *arXiv preprint arXiv:2106.07039*, 2021.

[Dai *et al.*, 2016] Hanjun Dai, Bo Dai, and Le Song. Discriminative embeddings of latent variable models for structured data. In *ICML*, pages 2702–2711, 2016.

[Deudon *et al.*, 2018] Michel Deudon, Pierre Cournut, Alexandre Lacoste, Yossiri Adulyasak, and Louis-Martin Rousseau. Learning heuristics for the tsp by policy gradient. In *CPAIOR*, 2018.

[Domingos and Richardson, 2001] Pedro Domingos and Matt Richardson. Mining the network value of customers. In *KDD*, pages 57–66, 2001.

[Fu *et al.*, 2021] Zhang-Hua Fu, Kai-Bin Qiu, and Hongyuan Zha. Generalize a small pre-trained model to arbitrarily large tsp instances. In *AAAI*, volume 35, pages 7474–7482, 2021.

[Gao *et al.*, 2016] Jie Gao, Golnaz Ghasemiesfeh, Grant Schoenebeck, and Fang-Yi Yu. General threshold model for social cascades: Analysis and simulations. In *EC*, pages 617–634, 2016.

[Ghasemiesfeh *et al.*, 2013] Golnaz Ghasemiesfeh, Roozbeh Ebrahimi, and Jie Gao. Complex contagion and the weakness of long ties in social networks: revisited. In *EC*, 2013.

[Girvan and Newman, 2002] Michelle Girvan and Mark EJ Newman. Community structure in social and biological networks. *PNAS*, 99(12):7821–7826, 2002.

[Goldenberg *et al.*, 2001] Jacob Goldenberg, Barak Libai, and Eitan Muller. Talk of the network: A complex systems look at the underlying process of word-of-mouth. *Marketing Letters*, 12(3):211–223, 2001.

[Granovetter, 1978] Mark Granovetter. Threshold models of collective behavior. *American Journal of Sociology*, 83(6):1420–1443, 1978.

[Graves *et al.*, 2016] Alex Graves, Greg Wayne, Malcolm Reynolds, Tim Harley, Ivo Danihelka, Agnieszka Grabska-Barwińska, Sergio Gómez Colmenarejo, Edward Grefenstette, Tiago Ramalho, John Agapiou, et al. Hybrid computing using a neural network with dynamic external memory. *Nature*, 538(7626):471–476, 2016.

[Hottung *et al.*, 2021] André Hottung, Yeong-Dae Kwon, and Kevin Tierney. Efficient active search for combinatorial optimization problems. In *ICLR*, 2021.

[Isella *et al.*, 2011] L. Isella, J. Stehlé, A. Barrat, C. Cattuto, J.-F. Pinton, and W. Van den Broeck. What's in a crowd? analysis of face-to-face behavioral networks. *J. Theor. Biol.*, page 166, 2011.

[Joshi *et al.*, 2019] Chaitanya K Joshi, Thomas Laurent, and Xavier Bresson. An efficient graph convolutional network technique for the travelling salesman problem. *arXiv preprint arXiv:1906.01227*, 2019.

[Kamarthi *et al.*, 2020] Harshavardhan Kamarthi, Priyesh Vijayan, Bryan Wilder, Balaraman Ravindran, and Milind Tambe. Influence maximization in unknown social networks: Learning policies for effective graph sampling. In *AAMAS*, pages 575–583, 2020.

[Kempe *et al.*, 2003] David Kempe, Jon Kleinberg, and Éva Tardos. Maximizing the spread of influence through a social network. In *KDD*, pages 137–146, 2003.

[Khalil *et al.*, 2017] Elias Khalil, Hanjun Dai, Yuyu Zhang, Bistra Dilkina, and Le Song. Learning combinatorial optimization algorithms over graphs. In *NeurIPS*, pages 6348–6358, 2017.

[Kim *et al.*, 2015] David A Kim, Alison R Hwong, Derek Stafford, D Alex Hughes, A James O'Malley, James H Fowler, and Nicholas A Christakis. Social network targeting to maximise population behaviour change: a cluster randomised controlled trial. *The Lancet*, 386(9989):145–153, 2015.

[Kool *et al.*, 2018] Wouter Kool, Herke van Hoof, and Max Welling. Attention,llearn to solve routing problems! In *ICLR*, 2018.

[Kool *et al.*, 2021] Wouter Kool, Herke van Hoof, Joaquim Gromicho, and Max Welling. Deep policy dynamic programming for vehicle routing problems. *arXiv preprint arXiv:2102.11756*, 2021.

[Kuhlman *et al.*, 2011] Chris Kuhlman, V Kumar, Madhav Marathe, S Ravi, D Rosenkrantz, Samarth Swarup, and Gaurav Tuli. A

bi-threshold model of complex contagion and its application to the spread of smoking behavior. In *Proceedings of the Workshop on Social Network Mining and Analysis (SNA-KDD 2011)*, 2011.

[Kwon *et al.*, 2020] Yeong-Dae Kwon, Jinho Choo, Byoungjip Kim, Iljoo Yoon, Youngjune Gwon, and Seungjai Min. Pomo: Policy optimization with multiple optima for reinforcement learning. *NeurIPS*, 33:21188–21198, 2020.

[Leskovec *et al.*, 2007a] Jure Leskovec, Lada A Adamic, and Bernardo A Huberman. The dynamics of viral marketing. *ACM Transactions on the Web (TWEB)*, 1(1):5–es, 2007.

[Leskovec *et al.*, 2007b] Jure Leskovec, Andreas Krause, Carlos Guestrin, Christos Faloutsos, Jeanne VanBriesen, and Natalie Glance. Cost-effective outbreak detection in networks. In *KDD*, pages 420–429, 2007.

[Li *et al.*, 2019] Hui Li, Mengting Xu, Sourav S Bhowmick, Changsheng Sun, Zhongyuan Jiang, and Jiangtao Cui. Disco: Influence maximization meets network embedding and deep learning. *arXiv preprint arXiv:1906.07378*, 2019.

[Lin *et al.*, 2015] Su-Chen Lin, Shou-De Lin, and Ming-Syan Chen. A learning-based framework to handle multi-round multi-party influence maximization on social networks. In *KDD*, pages 695–704, 2015.

[Lin, 1992] Long-Ji Lin. Self-improving reactive agents based on reinforcement learning, planning and teaching. *Machine learning*, 8(3-4):293–321, 1992.

[Manchanda *et al.*, 2020] Sahil Manchanda, Akash Mittal, Anuj Dhawan, Sourav Medya, Sayan Ranu, and Ambuj Singh. Gcomb: Learning budget-constrained combinatorial algorithms over billion-sized graphs. *NeurIPS*, 33, 2020.

[Mao *et al.*, 2019] Hongzi Mao, Malte Schwarzkopf, Shaileshh Bojja Venkatakrishnan, Zili Meng, and Mohammad Alizadeh. Learning scheduling algorithms for data processing clusters. In *SIGCOMM*, pages 270–288, 2019.

[Mazyavkina *et al.*, 2021] Nina Mazyavkina, Sergey Sviridov, Sergei Ivanov, and Evgeny Burnaev. Reinforcement learning for combinatorial optimization: A survey. *Computers & Operations Research*, page 105400, 2021.

[Mnih *et al.*, 2013] Volodymyr Mnih, Koray Kavukcuoglu, David Silver, Alex Graves, Ioannis Antonoglou, Daan Wierstra, and Martin Riedmiller. Playing atari with deep reinforcement learning. *arXiv preprint arXiv:1312.5602*, 2013.

[Nazari *et al.*, 2018] Mohammadreza Nazari, Afshin Oroojlooy, Martin Takáč, and Lawrence V Snyder. Reinforcement learning for solving the vehicle routing problem. In *NeurIPS*, pages 9861–9871, 2018.

[Ou *et al.*, 2021] Han-Ching Ou, Haipeng Chen, Shahin Jabbari, and Milind Tambe. Active screening for recurrent diseases: A reinforcement learning approach. In *AAMAS*, pages 992–1000, 2021.

[Qiu *et al.*, 2019] Wei Qiu, Haipeng Chen, and Bo An. Dynamic electronic toll collection via multi-agent deep reinforcement learning with edge-based graph convolutional networks. In *IJCAI*, pages 4568–4574, 2019.

[Romero *et al.*, 2011] Daniel M Romero, Brendan Meeder, and Jon Kleinberg. Differences in the mechanics of information diffusion across topics: Idioms, political hashtags, and complex contagion on twitter. In *WWW*, pages 695–704, 2011.

[Rossi and Ahmed, 2015] Ryan A. Rossi and Nesreen K. Ahmed. The network data repository with interactive graph analytics and visualization. In *AAAI*, 2015.

[Schaul *et al.*, 2016] Tom Schaul, John Quan, Ioannis Antonoglou, and David Silver. Prioritized experience replay. In *ICLR*, 2016.

[Schoenebeck and Tao, 2017] Grant Schoenebeck and Biaoshuai Tao. Beyond worst-case (in) approximability of nonsubmodular influence maximization. In *WINE*, pages 368–382. Springer, 2017.

[Schoenebeck and Tao, 2019] Grant Schoenebeck and Biaoshuai Tao. Beyond worst-case (in) approximability of nonsubmodular influence maximization. *ACM Transactions on Computation Theory*, 11(3):1–56, 2019.

[Schoenebeck *et al.*, 2020] Grant Schoenebeck, Biaoshuai Tao, and Fang-Yi Yu. Think globally, act locally: On the optimal seeding for nonsubmodular influence maximization. *arXiv preprint arXiv:2003.10393*, 2020.

[Shapley, 2016] Lloyd S Shapley. *17. A value for n-person games*. Princeton University Press, 2016.

[Tang *et al.*, 2015] Youze Tang, Yanchen Shi, and Xiaokui Xiao. Influence maximization in near-linear time: A martingale approach. In *SIGMOD*, pages 1539–1554, 2015.

[Tian *et al.*, 2020] Shan Tian, Songsong Mo, Liwei Wang, and Zhiyong Peng. Deep reinforcement learning-based approach to tackle topic-aware influence maximization. *Data Science and Engineering*, pages 1–11, 2020.

[Ugander *et al.*, 2012] Johan Ugander, Lars Backstrom, Cameron Marlow, and Jon Kleinberg. Structural diversity in social contagion. *PNAS*, 109(16):5962–5966, 2012.

[Van Hasselt *et al.*, 2016] Hado Van Hasselt, Arthur Guez, and David Silver. Deep reinforcement learning with double q-learning. In *AAAI*, volume 30, 2016.

[Vaswani *et al.*, 2017] Ashish Vaswani, Noam Shazeer, Niki Parmar, Jakob Uszkoreit, Llion Jones, Aidan N Gomez, Łukasz Kaiser, and Illia Polosukhin. Attention is all you need. *NeurIPS*, 30, 2017.

[Veličković *et al.*, 2018] Petar Veličković, Guillem Cucurull, Arantxa Casanova, Adriana Romero, Pietro Liò, and Yoshua Bengio. Graph attention networks. In *ICLR*, 2018.

[Wang *et al.*, 2012] Chi Wang, Wei Chen, and Yajun Wang. Scalable influence maximization for independent cascade model in large-scale social networks. *Data Mining and Knowledge Discovery*, 25:545–576, 2012.

[Watkins and Dayan, 1992] Christopher JCH Watkins and Peter Dayan. Q-learning. *Machine learning*, 8(3-4):279–292, 1992.

[Watkins, 1989] Christopher John Cornish Hellaby Watkins. Learning from delayed rewards. *PhD thesis, University of Cambridge*, 1989.

[Wilder *et al.*, 2021] Bryan Wilder, Laura Onasch-Vera, Graham Diguiseppi, Robin Petering, Chyna Hill, Amulya Yadav, Eric Rice, and Milind Tambe. Clinical trial of an ai-augmented intervention for hiv prevention in youth experiencing homelessness. In *AAAI*, pages 14948–14956, 2021.

[Zhang *et al.*, 2020] Cong Zhang, Wen Song, Zhiguang Cao, Jie Zhang, Puay Siew Tan, and Xu Chi. Learning to dispatch for job shop scheduling via deep reinforcement learning. *NeurIPS*, 33, 2020.

[Zhu *et al.*, 2021] Hang Zhu, Varun Gupta, Satyajeet Singh Ahuja, Yuandong Tian, Ying Zhang, and Xin Jin. Network planning with deep reinforcement learning. In *SIGCOMM*, pages 258–271, 2021.

A Proof of Theorem 1

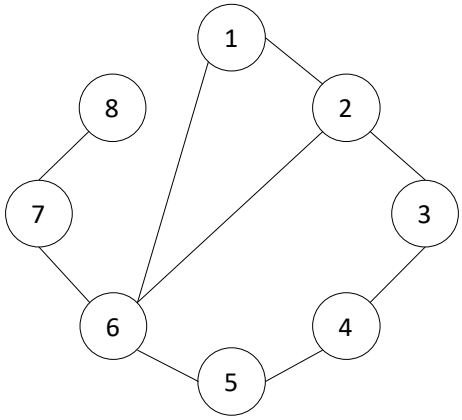

Proof. We prove it with a counter example by re-using the network depicted in Figure 2. Again, we set $p_0 = 1, p_1 = 0$ in Eq.(1), activation threshold $K = 3$. We re-place the figure in the above for ease of reference.

We first construct two sets, where the first $S = \{1\}$ is a singleton, and the second set $S' = \{1, 3\}$ is a superset of S: $S \subset S'$. Let the new node $v = 6$. Therefore, we have the following total influence values. Here we omitted the G notation in the influence for clarity.

$$\sigma(S) = \sigma(\{1\}) = 1$$
$$\sigma(S') = \sigma(\{1, 3\}) = 2$$
$$\sigma(S \cup \{v\}) = \sigma(\{1, 6\}) = 2$$
$$\sigma(S' \cup \{v\}) = \sigma(\{1, 3, 6\}) = 4$$

Here the total influence of $S \cup \{v\}$ is 4 because node 2 is activated (as the activated neighbors reaches the threshold K). Therefore,

$$\sigma(S \cup \{v\}) - \sigma(S) < \sigma(S' \cup \{v\}) - \sigma(S')$$

which violates the submodularity definition in Definition 1. □

B Hyperparameter values and ranges

For Greedy and DPIM, the number of iterations to estimate the expected influence spread of a given seed set is set to 50. For our impmentation of DPIM [Angell and Schoenebeck, 2017], the hierarchical decomposition tree of the original graph is constructed using the Jaccard Similarity metric.

For RL4IM and RL4IM-CC, certain hyperparameter values are the same across all the networks. These include: the maximal number of training time steps of all the networks are set to 5000 after searching within [2000, 8000]. The exploration probability ε and solution filtering probability ε both uniformly decrease from 0.99 at training step $t = 0$ to 0.01 at $t = 4000$, and stays at 0.01 afterwards. We just set them as default values without extra tuning. We use double DQN [Van Hasselt *et al.*, 2016] as the underlying Q-learning part, where the target update networks starts updating at $t = 2500$ and updates every 20 time steps afterwards. We also use the n-step Q [Watkins, 1989] where n is set to 5 after searching within [1, 8]. Learning rate is set to 0.0005 after tuning within [0.0001, 0.01]. The batch size is set to 32 after searching within [8, 64]. For PER, the hyperparameters ϵ, α are set to 0.01 and 0.6 by default without tuning. For the graph representation, we are using the GAT [Veličković *et al.*, 2018] with 8 attention heads. There are some other parameters that are tuned for each network: the reward shaping weight ω is tuned within $\{0.001, 0.005, 0.01\}$. The 3 variants of priority metrics for PER are tuned in each network. The weight β is tuned within $\{0.5, 1, 2\}$.

For the stochastic propagation setting, the number of iterations to get the expected influence at evaluation time for all methods is set to 1000.

Table 2: Statistics of the 9 networks.

Network	$\|V\|$	$\|E\|$	Ave. degree	density
CHANGE	53	65	2.5	0.0472
DC	41	56	2.7	0.0683
DOSIM	40	45	2.2	0.0577
MFP	72	112	3.1	0.0438
SPY	67	129	3.9	0.0583
Football	115	613	10.7	0.0935
Polbooks	105	441	8.4	0.0808
India	202	692	6.9	0.0341
Exhibition	410	2765	13.5	0.0330

C Description of the networks

Networks **CHANGE-SPY** are real-world social networks collected from the homeless youth shelter in the city of Los Angeles. The edges represent friendship relationships among the youth. **Football** [Girvan and Newman, 2002] is a network among different teams of the 2000 United States college football season, where nodes represent teams (identified by their college names) and edges represent regular-season games between the two teams they connect **India** [Banerjee *et al.*, 2013] is a network collected from one of the villages in India by households surveying. The edges represent the real world social contact. **Polbooks** [Rossi and Ahmed, 2015] is a network of books about US politics sold by Amazon.com. Edges represent frequent co-purchasing of books by the same buyers. **Exhibition** [Isella *et al.*, 2011] is a physical contact network representing the face-to-face contacts of people in a large event. The statistics of the networks are listed in Table 2.

D Mixed integer programming formulation

We can formulate the following mixed-integer program for CCIM in the deterministic case ($p = 1$). Let $N(v)$ be the neighborhood of node v and let L be the number of time steps over which the MIP will evaluate the contagion. When L is sufficiently large (e.g., the number of nodes in the graph), we are guaranteed that the MIP objective will match the CCIM objective exactly; otherwise the MIP objective provides a lower bound. We found that setting $L = 10$ was empirically sufficient to ensure an exact match between the MIP and CCIM objectives.

$$\max \sum_{v} x_v^L \tag{8}$$

$$\text{s.t.} \quad x_v^0 \leq \frac{1}{K} \sum_{u \in N(v)} s_u \tag{9}$$

$$x_v^t \leq \frac{1}{K} \sum_{u \in N(v)} x_u^{t-1}, t = 1...L \tag{10}$$

$$\sum_{v \in V} s_v \leq T \tag{11}$$

In the stochastic case $0 < p < 1$, we can extend the above MIP using sample average approximation. Specifically, we can sample a number of different realizations of $N(v)$ by including each of v's neighbors in the set of realized active edges with probability p. For each of these samples, we can duplicate the x variables and then average across scenarios in the objective. However, we found that empirically, this approach resulted in impracticably long running times (> 12 hours) due to the increase in the number of variables.

E Compare selected seeds of Greedy and RL4CCIM

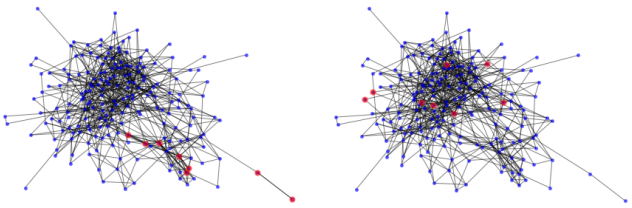

(a) Greedy (b) RL4CCIM

Figure 6: Visualization of seeds selected by Greedy and RL4CCIM in the India village network. Red nodes are the selected seeds. Greedy selects arbitrary seeds in low-density areas whereas RL4CCIM concentrates on high-density clusters.

The comparison is in Figure 6. Interestingly, we can see that Greedy selects nodes in the very margins of the network, where some nodes do not even belong to the effective candidate set $\mathcal{A}$. This is because at the first few steps ($t < K$), any node has a zero effective marginal reward, and thus arbitrary nodes are selected at the beginning. After that, it greedily expands the seed set along the initial set of seeds. This leads to arbitrarily bad solution. On the contrary, to initialize the first set of activated nodes, the solution selected by RL4CCIM tend to be concentrated in local communities to form a threshold number of neighbors. This is consistent with the insight of a good strategy in [Schoenebeck *et al.*, 2020]. Moreover, the reward shaping component encourages the policy to avoid the low-potential nodes even at initial time steps.